Available online at www.sciencedirect.com
SCIENCE DIRECT®
ELSEVIER
International Journal of Mechanical Sciences 47 (2005) 1442–1454
International Journal of MECHANICAL SCIENCES
www.elsevier.com/locate/ijmecsci

Determining probability of mission success when using deep penetration weapons

Ravi C. Penmetsa*

Department of Mechanical and Materials Engineering, Wright State University, Dayton, OH 45435, USA

Received 25 August 2004; received in revised form 20 April 2005; accepted 30 April 2005
Available online 15 June 2005

Abstract

This paper presents the methodology for a system reliability analysis that can determine the probability of mission success of the destruction of buried concrete targets using deep penetration weapons. The success of the mission depends on various parameters, such as the properties of the target, the velocity and structural strength of the missile, the impact angle, etc., as well as other military scenarios. However, this paper only considers the structural design aspects. In this paper, analytical equations for the depth of penetration and buckling strength of the missile are used to demonstrate an efficient system reliability analysis methodology. These equations are also used to determine the sensitivity of mission success to various parameters. A discussion on the selection of parameters to maximize the mission success is also presented.

Keywords: Deep penetration weapon; System reliability; Mission success; Probability

1. Introduction

Most strategic targets are buried underground and their destruction is important for the overall success of a war. Destruction of these targets with a minimum number of missiles is economical to the military, more lethal, and beneficial from a strategic point of view. The destruction of these

*Tel.: +1 937 775 5089; fax: +1 937 775 5009.
E-mail address: pravi@cs.wright.edu.

0020-7403/$ - see front matter © 2005 Elsevier Ltd. All rights reserved.
doi:10.1016/j.ijmecsci.2005.04.014

targets is usually measured through the damage caused by the striking missiles. Usually a full penetration of the missile into the target is considered as the complete destruction of the target and would represent a successful mission. Investigators in the past have proposed various empirical [1,2], analytical [3], and numerical [4,6] procedures for the estimation of penetration depths under a given missile impact. These predictions were deterministic, whereas the actual penetration problem has significant uncertainties in its variables. This shows that the missile penetration into a target is a random event, while the past work [7,8] shows only a deterministic approach. In this paper, a detailed system reliability analysis of these missions is performed by considering the depth of penetration and the structural integrity of the missile as the criteria. The various expressions required to determine the depth of penetration in crater and tunnel regions were derived based on the methodology obtained in the literature [1,5]. These penetration depths have been used in conjunction with the buckling criteria of the missile. The sensitivity of mission success to various uncertain parameters is examined and the important, controllable parameters are identified. A robust configuration for maximizing the mission success is presented that is based on these parameters.

1.1. Reliability analysis

A fundamental problem in structural reliability analysis is the computation of the multi-dimensional integral

$$p_f = \int_{\Omega} f_x(X)\mathrm{d}X, \tag{1}$$

where $f_x(X)$ denotes the joint probability density function (PDF) of the vector of basic random variables and $X = (x_1, x_2, \ldots, x_n)^{\mathrm{T}}$ represents uncertain quantities such as loads, geometry, material properties, and boundary conditions. This equation is also called the convolution integral because convolution of the individual PDF over the failure domain would result in the joint PDF of the response. Furthermore, Ω is the failure region modeled by the limit-state function or the performance function $g(X)$. The failure region is defined by $g(X) \leqslant 0$ and p_f is the probability of structural failure.

In practice, it is usually difficult to construct the joint density function $f_x(X)$ and/or to determine each individual density function due to the scarcity of statistical data. Even in the case for which the statistical information may be sufficient to determine these functions, it is often impractical to perform the multi-dimensional numerical integration over the failure region Ω. These difficulties have motivated the development of various reliability approximation methods within the past 2 decades.

Among the approximation methods available, the most common one is the first-order reliability method (FORM) [9]. In this method the limit-state is approximated by the tangent plane at the most probable failure point (MPP). The MPP is a point on the limit-state in the normalized domain that has a maximum probability density. FORM is most accurate when the random variables are normally distributed and the limit-state function is nearly linear in the neighborhood of the MPP. However, if the failure surface has a high nonlinearity, which is the case in depth of penetration situations, the failure probability estimated using the safety index β by FORM gives

inaccurate results. In order to improve the accuracy, high fidelity methods [10–12] have to be applied.

The failure probability of the system, however, is the integration of the joint PDF over the entire failure region obtained by the intersection of all the limit-states, as opposed to a single limit-state in component reliability analysis. Structural systems are classified as series systems and parallel systems [13]. A series system is one in which if even one component fails, the whole system fails. These systems are also called weakest-link systems. In the case of parallel systems, the system survives even if one or more of the components have failed. The system fails to function satisfactorily only when every component has failed. Parallel systems are also called redundant systems. In the present work, a series system is considered in which the mission fails if the any of the criteria is not satisfied.

1.2. Solving the convolution integral in intervals

For solving the convolution integral, the function, based on which integral is evaluated, must be available as a closed-form and separable equation. The procedure for solving the convolution is discussed in detail by Penmetsa and Grandhi [12]. As a single approximation cannot model a highly nonlinear joint failure region, several function approximations are constructed over the entire domain represented by the uncertain variables.

Let us suppose that the failure probability of the structural system is governed by two limit-state criteria, $g_1(x_1, x_2) \leqslant 0$ and $g_2(x_1, x_2) \leqslant 0$, where x_1 and x_2 are the random variables, as shown in Fig. 1. These limit-states intersect at a point where $x_1 = x_0$. The joint failure region comprises

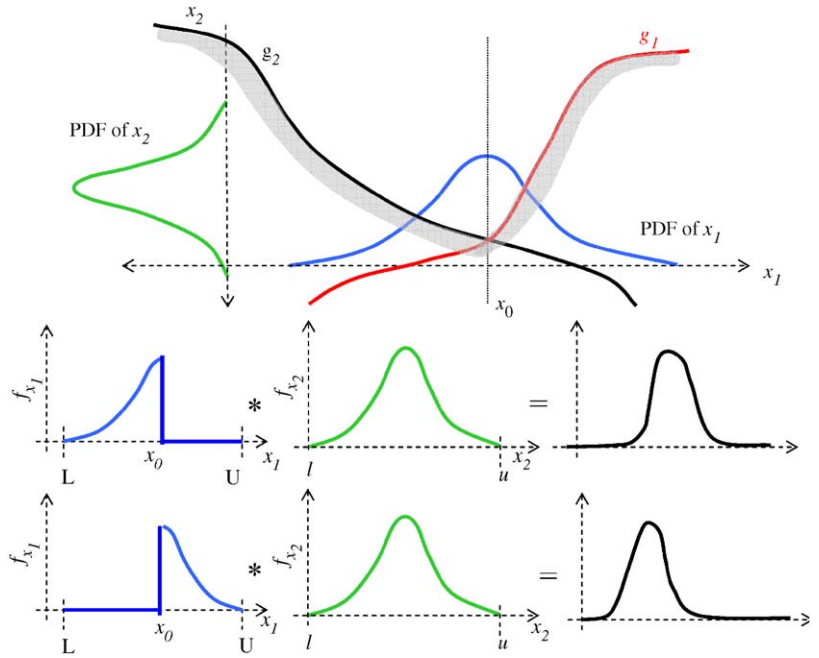

Fig. 1. Convolution in intervals.

of the part of g_2 where $x_1 < x_0$ and the part of g_1 where $x_1 > x_2$. Based on this information, the joint failure region is divided into two different integrals, as shown in Eq. (2).

$$\int\int_{\Omega} f_X(X)\,\mathrm{d}X = \int_{-\infty}^{x_0}\int_{-\infty}^{\infty} f_X(X)\,\mathrm{d}x_2\,\mathrm{d}x_1 + \int_{x_0}^{\infty}\int_{-\infty}^{\infty} f_X(X)\,\mathrm{d}x_2\,\mathrm{d}x_1. \tag{2}$$

The two integrals in Eq. (2) can be solved separately. The PDF of x_1, when $x_1 < x_0$, is convoluted with the PDF of x_2, based on g_2, to evaluate the first integral, since only g_2 represents the system failure surface. The PDF of x_1, when $x_1 > x_0$ is convoluted based on g_1 for the other integral. The final PDF of the system is a combination of these two integrals.

In a problem with more than two random variables, the intersection of the limit-states is not a point but a surface (hyperplane), making it difficult to split the PDFs, as shown in Fig. 1. Therefore, the entire design space is divided into regions and the convolution integral is solved for each region separately. The convolution integral is then written as the sum of integrals over all the regions as

$$\int\int_{\phi}\int f_x(X)\mathrm{d}X = \int\int_{\phi_1}\int f_x(X)\mathrm{d}X + \int\int_{\phi_2}\int f_x(X)\mathrm{d}X + \ldots. \tag{3}$$

As shown in Fig. 2, the entire design space is divided into several regions such that the joint failure region can be modeled with approximate models that are accurate within that region. The convolution integral is divided into several integrals as shown in Eq. (3). These integrals are then solved using fast fourier transforms (FFT), based on the approximate model that is accurate within that region. Finally, all the PDFs of the various models are added to result in the PDF of the structural system.

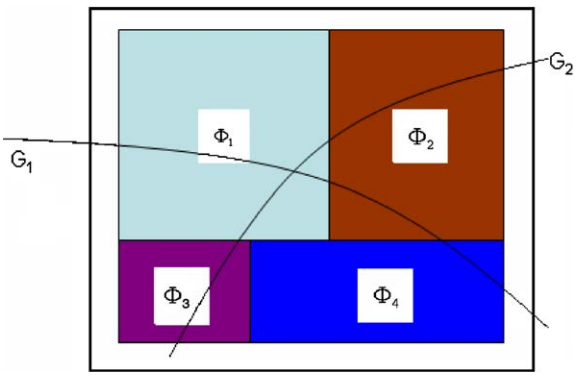

Fig. 2. Multiple approximations modeling different failure regions.

1.2.1. Numerical example for system reliability

A cantilever beam, as shown in Fig. 3, subjected to a tip load of 444.82 N, is selected to demonstrate the system reliability method used in this paper. Two failure criteria for the structure were considered: (i) the displacement at the tip of the beam should be less than 0.002 m, as shown below, and (ii) the stress in the beam should be less than 34 MPa.

$$\text{Displacement limit-state} \quad g_1(X) = \frac{4PL^3}{Ebh^3} - 0.002 \leqslant 0$$

$$\text{Stress limit-state} \quad g_2(X) = \frac{12PL}{bh^2} - 34 \times 10^6 \leqslant 0$$

where L, b, h are the length, width, and height of the beam, which are all taken as random variables. The length of the beam is assumed to be normally distributed with a mean value of 0.762 m and a standard deviation of 0.0762 m. The width and height of the beam were both assumed to be normally distributed with mean values of 0.0635 m and standard deviations of 0.00635 m.

As the limit-state functions are available as a closed-form expressions in terms of the random variables, there is no need to construct approximations of each of the limit-state functions. Using these closed-form expressions, several points were sampled on the joint failure region. These sampled points were used in the construction of multiple response surface models to represent the joint failure region. The design space is divided into smaller domains such that the response surface model captures the joint failure region accurately within that domain. The convolution integral is solved over the entire design space to obtain the failure probability of the system.

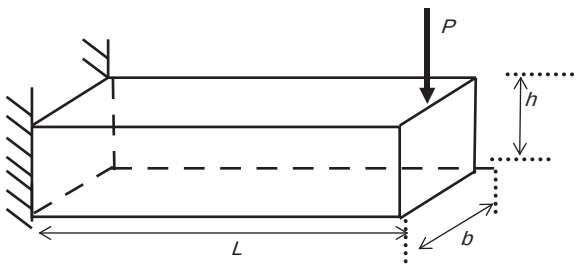

Fig. 3. Cantilever beam.

Table 1
Comparison of results obtained with Monte Carlo simulation

Methodology	System failure probability	% Difference
Monte Carlo simulation	0.0091	—
RSM + FFT	0.0093	2.19
First-order series bounds	0.0089–0.0111	−2.19–21.98

Table 1 illustrates the accuracy of the methodology in the prediction of the failure probability of the system. The error in the failure probability estimated by the proposed methodology to that of Monte Carlo simulation is around 2.19%. One million evaluations of the limit-state functions were used in the estimation of the failure probability using the Monte Carlo simulations.

2. Expression for depth of penetration and buckling load

Depth of penetration is a highly nonlinear expression that depends on various parameters, such as missile velocity, material properties, angle of impact, etc. Various assumptions have been used to derive the expression for depth of penetration based on the information available in the literature. It is assumed that the impact is normal and axi-symmetric, and that the missile does not carry a warhead. This ignores the explosion condition in determining the depth of penetration. Moreover, the missile is considered as rigid in order to determine the depth of penetration; since this is not the case, the buckling constraint is added to restrict maximum force on the missile.

A missile that has an initial velocity v_0 penetrates into the geomaterial experiencing an axial resting force F_A at the nose, due to the soil medium. This force for a given missile configuration and geomaterial lay-up (Fig. 4) were obtained from Ref. [5].

$$F_A = \alpha\pi a^2 v_A \tan(\theta)\sqrt{K\rho_g}, \tag{4}$$

where α is the slope of the linear fit to the curves plotted between σ_r/K and $v_A \tan(\theta)/\sqrt{K\rho_g}$, a is the missile shank radius, v_A is the axial velocity of the missile at any time, θ is an equivalent half cone angle equal to $\tan^{-1}\left(1/\sqrt{4\Psi - 1}\right)$, Ψ is the caliber radius of the missile nose, K is the bulk modulus of geomaterial, and ρ_g is the initial mass density of geomaterial.

By using Newton's second law, the equation of motion of the missile with mass m can be written as $m(d^2Z_g/dt^2) = -F_A$, where Z_g is the depth of penetration at any time t. By integrating this

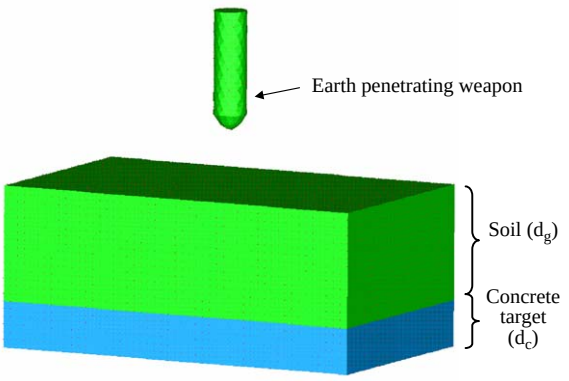

Fig. 4. Generic model of a deep penetration problem.

equation of motion with initial conditions we can obtain the following expressions:

$$z_g = \frac{mv_0}{\alpha\pi ta^2 \tan(\theta)\sqrt{K\rho_g}} \times \left\{1 - \mathrm{Exp}\left[\frac{-\alpha\pi ta^2 \tan(\theta)\sqrt{K\rho_g}}{m}\right]\right\}, \tag{5}$$

$$v_A = \frac{\mathrm{d}z_g}{\mathrm{d}t} = v_0 \,\mathrm{Exp}\left[\frac{-\alpha\pi ta^2 \tan(\theta)\sqrt{K\rho_g}}{m}\right]. \tag{6}$$

By using Eqs. (5) and (6) we can obtain the velocity of missile (v_s) striking the concrete target where $Z_g = d_g$,

$$v_s = v_0\left[1 - \frac{d_g\alpha\pi ta^2 \tan(\theta)\sqrt{K\rho_g}}{mv_0}\right]. \tag{7}$$

When a missile impacts a buried target with a velocity v_A it creates a conical-shaped crater region with a depth approximately equal to twice the missile shank diameter, $4a$, followed by a cylinder-shaped tunnel region with a diameter nearly equal to the shank diameter, $2a$, as shown in Fig. 5. Expressions for these depths are given below:

$$z_{crater} = \frac{2}{\sqrt{\pi a}} v_0\left\{1 - \frac{d_g\alpha\pi a^2 \tan(\theta)\sqrt{K\rho_g}}{mv_0}\right\} \times \sqrt{\frac{m + 4\pi a^3 N\rho_c}{Sf_c + N\rho_c v_0^2\left[1 - \left(d_g\alpha\pi a^2 \tan(\theta)\sqrt{K\rho_g}\right)/mv_0\right]^2}} \tag{8}$$

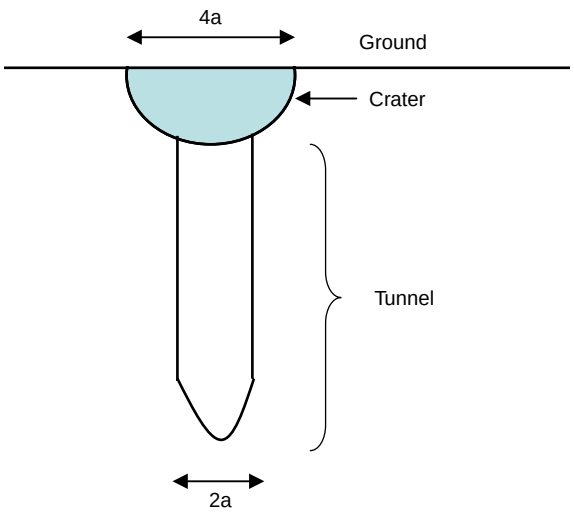

Fig. 5. Cartner and tunnel formation for a group penetrating missile.

$$z_{tunnel} = 4a + \frac{m}{2\pi a^2 N \rho_c} \times \ln\left(1 + \frac{N\rho_c(m^2 v_0^2 - 2mv_0 d_g \alpha \pi a^2 \tan(\theta)\sqrt{K\rho_g} + d_g^2 \alpha^2 \pi^2 a^4 \tan^2(\theta) K\rho_g - 4\pi a^3 m S f_c)}{(m^2 S f_c + 4\pi a^3 m N \rho_c S f_c)}\right), \tag{9}$$

where d_g is the depth of target in the geomaterial, f_c is the compressive strength of concrete, ρ_c is the density of concrete, and N and S are dimensionless constants. By using these expressions, the depth of penetration of the missile can be obtained as follows:

$$\text{Missile depth of penetration } G_1 = \begin{cases} \text{If } z_{crater} > 4a & \text{then } G_1 = z_{tunnel}, \\ \text{Else} & G_1 = z_{crater}. \end{cases} \tag{10}$$

The second limit-state is the buckling constraint on the missile. The missile is assumed to be a flexible structure and its critical buckling load is modeled using the following equation:

$$P_{Cr} = \frac{E(\pi a^4/4)\pi^2}{(1.2L)^2}. \tag{11}$$

By using the maximum force expression from Eqs. (4) and (11), we can easily formulate the second limit-state equation to maintain structural integrity.

3. Problem definition

For the purpose of performing a system reliability analysis, a missile of mass 182 kg and shank radius 0.0825 m with impact velocity 411 m/s has been selected. These data are obtained from Ref. [5]. Material properties of the geomaterial and concrete are given in Table 2. The selected

Table 2
Uncertain variable information

Random variable	Distribution	Mean	COV	Reference
Mass of the missile, m	Lognormal	182 kg	0.05	[5]
Missile shank radius, a	Normal	0.0825 m	0.05	[5]
Caliber radius head, Ψ	Normal	9.25	0.05	[5,2]
Missile impact velocity, v_0	Extreme type 1	411 m/s	0.10	[5]
Geomaterial bulk modulus, K	Lognormal	9520 Mpa	0.15	[5]
Density of geomaterial, ρ_g	Lognormal	1970 kg/m^3	0.15	[5]
Slope of linear fit, α	Normal	0.80	0.10	[5]
Depth of target in geomaterial, d_g	Normal	1.0 m	0.05	Assumed
Non-dimensional parameter, S	Normal	11.10	0.15	[2]
Density of concrete, ρ_c	Lognormal	2000 kg/m^3	0.10	[2]
Concrete compressive strength, f_c	Lognormal	40.0 Mpa	0.10	[2]
Thickness of concrete target, d_c	Normal	0.50 m	0.05	Assumed
Elastic modulus of missile, E	Normal	100 GPa	0.10	Depleted uranium

configuration is considered to be nominal and a certain coefficient of variation (COV) is assigned for all of the uncertain parameters. This COV is the measure of uncertainty; and, the higher this value, the higher is the variation in the parameter.

Based on the uncertain variables defined in the table, the reliability of the mission (penetration into the concrete target) is determined to be 42.37%. This would be the final reliability of the mission if the missile was a rigid block. However, since the missile is susceptible to buckling the reliability of the missile is determined using the second constraint discussed above. This value is determined as 96.38%, which means that there is relatively low probability of the missile buckling during the mission. However, the system reliability is of interest in this work and this can be obtained using the above-discussed methodology. The entire domain represented by uncertain variables is modeled using eight response surfaces that were constructed using the Latin hypercube sampling method with 60 data points. Therefore, 480 data points were required to model the response surfaces that were used in the analysis.

These response surfaces were used to determine the range of integrals in Eq. (3) and FFT is used to evaluate the integrals. By using this method, the system reliability is determined to be 40.46%. There is a 5% drop in the reliability of the system by just considering the buckling constraint. Therefore, this clearly indicates that the weapon system design is a highly probabilistic event and deterministic techniques do not produce optimum configurations.

In Fig. 6, we can see the PDF of the depth of penetration, which is clearly skewed to the left of 2.0. Due to the shape of the distribution, a small change in the limit of the penetration depth would move a large area under the PDF into the failure or safe direction, thereby making it very sensitive. Therefore, one can determine that the PDF is most sensitive to the depths of the geomaterial and concrete, among other things.

There are numerous parameters that can be controlled to determine the configuration that maximizes the mission success. In order to perform design optimization, information about the sensitivity of mission success to these parameters is important. The following section discusses the sensitivities of various parameters to the mission success.

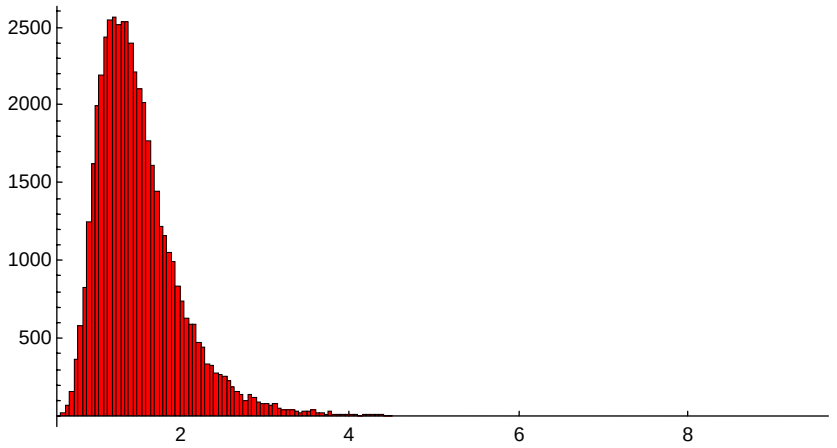

Fig. 6. PDF of depth of penetration.

4. Sensitivity of mission success

In order to determine the parameters that are most sensitive to the mission success, the sensitivity of the COV of each of these variables is examined. Only the parameters that result in at least 5% variation in the mission success rate are discussed below.

- *Mission success vs. missile shank radius*:
  Fig. 7 shows the relationship between the probability of mission success and the missile shank radius COV. Clearly, as the COV increases the probability of success decreases (about 22%) due to the fact that there are more realizations of a lower shank radius, which would not penetrate into the target. The lower shank radius results in more failures due to the violation of the buckling constraint. In this particular case the buckling constraint would drive the system reliability until a point where the shank radius is large enough and that more force is required to penetrate than what is available from the impact. Therefore, tight control of the missile shank radius is required in order to maintain a high rate of success.
- *Mission success vs. missile elastic modulus*:
  Fig. 8 shows the rate of decrease of the probability of mission success with respect to the variation in the elastic modulus. Clearly, the 8% decrease in this case can also be attributed to the increase in the number of missiles with lower elastic modulus, which causes them to buckle

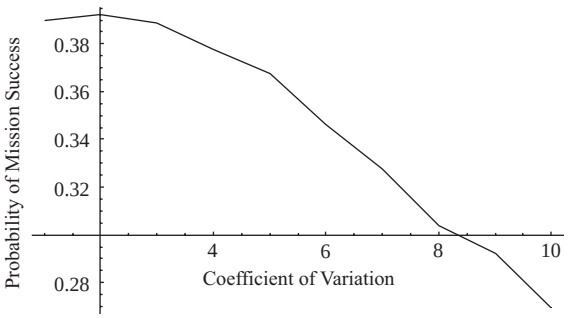

Fig. 7. Mission success vs. missile shank radius.

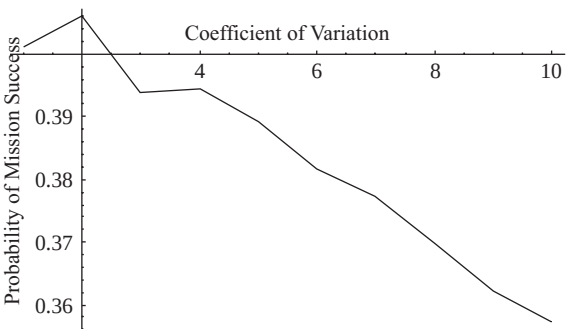

Fig. 8. Mission success vs. missile elastic modulus.

before the mission is complete. The bump in the plot is due to the convergence of the system probability solution at certain values of COV. Even though modulus of elasticity was considered as a random variable military applications can dictate a tighter tolerance due to available resources. Therefore, this 8% decrease can easily be avoided by specifying required tolerances on a modified nominal value. Since the overall trend can be clearly seen from the figure, more analyses were not performed to recreate the curve.

- *Mission success vs. missile mass*:
  Variation in the missile mass resulted in about 6.5% of variation in the probability of success. This did not prove to be that significant in the design process, considering the variations due to other parameters. Therefore, any changes in the mass of the missile due to the change in contents would not affect the mission drastically. However, it is still a parameter that needs to be monitored due to its tendency to lower the mission success rate. The higher mass would result in larger kinetic energy of the missile as it hits the ground, thereby increasing the final impact velocity. This impact velocity is responsible for the impact force from conservation of momentum principle. Therefore, when the mass was increased the impact force increased and the weapon buckled, leading to a failed mission (Fig. 9).
- *Mission success vs. velocity of the missile*:
  It can be seen from Fig. 10 and other results that this is the parameter that affects the mission success the most. There is about a 38% increase in the rate of success as the variation of velocity

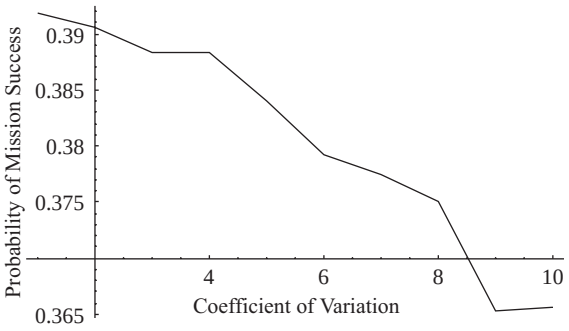

Fig. 9. Mission success vs. mass of the missile.

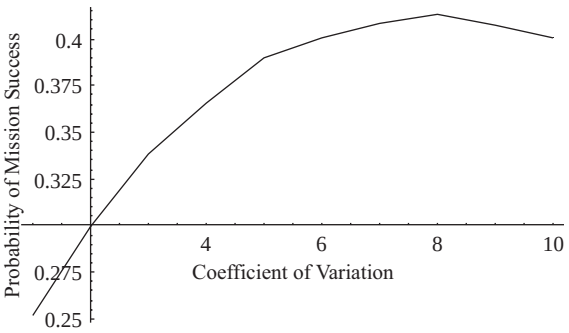

Fig. 10. Mission success vs. velocity of the missile.

increases from a low value to high value. This is due to the fact that the velocity is defined using an extreme value distribution that had a skewness coefficient (third moment) of 1.14, which means that the data is skewed to the right of the mean. Therefore, as the variation increases there are more and more realizations of velocity that are on the higher end, which leads to a deeper penetration. This can be clearly seen in Fig. 11, where PDFs for increasing variation are shown. The PDF that is spread the most represents a 20% COV, the tall PDF represents a 5% COV, and the third PDF representing 10% COV. From these PDFs we can see that the higher velocities are more probable when the COV increases, which results in improved mission success.

- *Mission success vs. non-dimensional parameter "S"*:
  In this case, the affect of a non-dimensional parameter that is used in the crater depth equation is examined and there is a 16% increase in the rate of success as the variance increased. Therefore, this parameter also plays an important role in the mission success. This type of parameter is usually considered as an uncontrollable parameter and its variation has to be determined with more confidence in order to effectively utilize other parameters that are controllable. This is a parameter that is used as a fudge factor to match the analytical results with the experimental data. Therefore, proper care must be given to determining this parameter, based on its sensitivity to the mission success (Fig. 12).

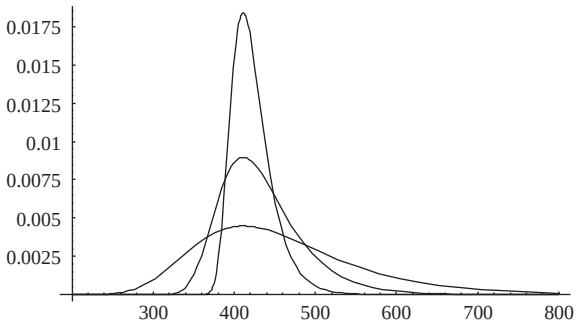

Fig. 11. PDF of missile velocity for different COV.

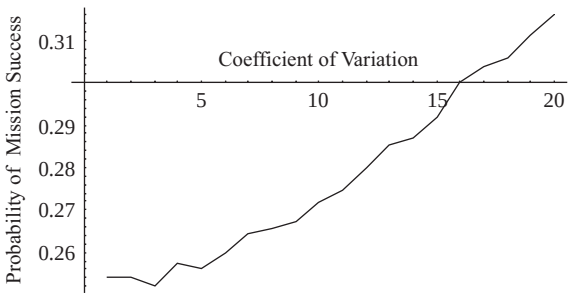

Fig. 12. Mission success vs. non-dimensional parameter "S".

5. Summary

Based on the analysis performed, it can be determined that the overall mission success rate is pretty low for the configuration that was selected. However, parameters that drastically affect the probability of mission success have been identified, and modifying their mean values will result in a higher success. The missile velocity was determined to have maximum positive sensitivity to the mission success probability and the missile shank radius had the maximum negative sensitivity. Therefore, a design that has a tighter control on the shank radius and allows for higher velocities would greatly improve the mission success probability. Based on the approach followed in this paper, more constraints can be added to the study and with the use of efficient system reliability methods presented here; one can determine the probability of success of an event. Usually, a mission involves multiple events that need to occur in a sequence, therefore, a realistic study would be one in which all of these events are modeled and simulated.

References

[1] Forrestal MJ, Altman BS, Cargile JD, Hanchak SJ. An empirical equation for penetration depth of Ogive-nose projectiles into concrete target. International Journal of Impact Engineering 1994;15(4):395–405.
[2] Frew DJ, Hanchak SJ, Green ML, Forrestal MJ. Penetration of concrete target with Ogive-nose steel rods. International Journal of Impact Engineering 1998;21(6):489–97.
[3] Forrestal MJ, Luk VK. Penetration into soil targets. International Journal of Impact Engineering 1992;12:427–44.
[4] Abbas H, Paul DK, Godbole PN, Nayak GC. Soft missile impact on rigid target. International Journal of Impact Engineering 1995;16(5/6):727–37.
[5] Forrestal MJ, Longscope DB, Norwood FR. A model to estimate forces on conical penetrators into dry porous rock. ASME Journal of Applied Mechanics 1981;48:25–9.
[6] Norwood FR, Sears MP. A nonlinear model for the dynamics of penetration into geological targets. ASCE Transactions 1982;49:26–30.
[7] Corbett CG, Reid SR, Johnson W. Impact loading of plates and shells by free flying projectiles: a review. International Journal of Impact Engineering 1996;18:141–230.
[8] Goldsmith W. Non-ideal projectile impact on targets. International Journal of Impact Engineering 1999;22:95–395.
[9] Hasofer AM, Lind NC. Exact and invariant second-moment code format. Journal of Engineering Mechanics Division-ASCE 1974;100(EM):111–21.
[10] Cia GQ, Elishakoff I. Refined second-order reliability analysis. Structural Safety 1994;14(4):267–76.
[11] Koyluoglu HU, Nielsen SRK. New approximations for SORM integrals. Structural Safety 1994;13(4):235–46.
[12] Penmetsa RC, Grandhi RV. Structural failure probability prediction using fast fourier transformations for high accuracy. Journal of Finite Elements in Analysis and Design 2003;39(5–6):473–86.
[13] Melchers RE. Structural reliability; analysis and prediction. Chichester, UK: Ellis Horwood; 1987. pp. 140–149.